

From Prompt Optimization to Multi-Dimensional Credibility Evaluation: Enhancing Trustworthiness of Chinese LLM-Generated Liver MRI Reports

Qiuli Wang¹, Jie Cheng², Yongxu Liu¹, Xingpeng Zhang³, Xiaoming Li², and Wei Chen²

¹Yu-Yue Pathology Research Center, Jinfeng Laboratory, Chongqing, China

²7T Magnetic Resonance Imaging Translational Medical Center, Department of Radiology,

Southwest Hospital, Army Medical University, Chongqing, China

³School of Computer Science and Software Engineering,

Southwest Petroleum University, Chengdu, China

Abstract—Background: Large language models (LLMs) have demonstrated promising performance in generating diagnostic conclusions from imaging findings, thereby supporting radiology reporting, trainee education, and quality control. However, systematic guidance on how to optimize prompt design across different clinical contexts remains underexplored. Moreover, a comprehensive and standardized framework for assessing the trustworthiness of LLM-generated radiology reports is yet to be established.

Purpose: This study aims to enhance the trustworthiness of LLM-generated liver MRI reports by introducing a Multi-Dimensional Credibility Assessment (MDCA) framework and providing guidance on institution-specific prompt optimization. The proposed framework is applied to evaluate and compare the performance of several advanced LLMs, including Kimi-K2-Instruct-0905, Qwen3-235B-A22B-Instruct-2507, DeepSeek-V3, and ByteDance-Seed-OSS-36B-Instruct, using the SiliconFlow platform.

Materials and Methods: Diagnostic conclusions were generated from liver MRI findings using several large language models (LLMs)—Kimi-K2-Instruct-0905 (Moonshot AI), Qwen3-235B-A22B-Instruct-2507 (Alibaba Group), DeepSeek-V3 (DeepSeek AI), and ByteDance-Seed-OSS-36B-Instruct (ByteDance)—via the SiliconFlow platform. The Multi-Dimensional Credibility Assessment (MDCA) framework was then applied to evaluate report trustworthiness across three dimensions: Semantic Coherence (SC), Diag-

nostic Correctness (DC), and Clinical Prioritization Alignment (CPA). Eleven prompt configurations were compared, encompassing combinations of role definition, core task specification, tiered diagnostic taxonomy (TOP system), mandatory verification items, report structure standards, imaging diagnostic principles, and example-based guidance. More than 15,000 institutional liver cancer reports were collected to validate the effectiveness of the prompts, quantify the contribution of each prompt component, and assess the performance of different LLMs.

Results: The proposed MDCA framework effectively evaluates the quality of LLM-generated reports. Using this framework, we found that optimizing prompt design notably improved diagnostic accuracy and clinical prioritization. Example-based prompts primarily enhanced semantic coherence, resulting in more fluent and logically consistent outputs. The benefit of including examples became more pronounced under limited computational resources, with approximately ten examples providing the optimal balance between performance and efficiency. Among the evaluated large language models, Kimi-K2-Instruct-0905 and DeepSeek-V3 achieved the best overall performance. Kimi-K2 obtained the highest composite score of 76.149, ranking first across all evaluation dimensions, while DeepSeek-V3 followed closely with 75.410, demonstrating similarly stable and reliable results.

Conclusion: Institution-specific prompt optimization and multi-dimensional credibility evaluation substantially improve the trustworthiness of LLM-

Corresponding authors: X. Li and W. Chen.

generated liver MRI reports. The proposed frameworks not only enhance reporting reliability and interpretability but also provide practical tools for radiology quality control and trainee education, supporting the safe and standardized integration of LLMs into clinical workflows.

Index Terms—Large Language Models, Prompt Engineering, Radiology Report Generation, Liver MRI, Credibility Assessment

I. INTRODUCTION

HEPATIC space-occupying lesions, particularly hepatocellular carcinoma (HCC), are highly prevalent in China and pose a significant clinical challenge [1]–[3]. Gadoxetate disodium (Gd-EOB-DTPA)-enhanced MRI has become an essential modality for lesion characterization, early detection, and surgical planning [4], [5]. At the Department of Radiology, The First Affiliated Hospital of Army Medical University in Chongqing, China, the demand for liver-specific MRI examinations continues to increase, placing growing pressure on radiologists. The large volume and complexity of imaging data frequently lead to a decline in report quality, manifesting as vague terminology, inconsistent interpretations, and suboptimal standardization.

The rapid advancement of Chinese large language models (LLMs)—such as Kimi-K2, Qwen3, DeepSeek-V3, and ByteDance-Seed—has created new opportunities for radiology report generation in native-language clinical practice [6]–[10]. These models exhibit strong capabilities in producing coherent, standardized, and stylistically consistent diagnostic narratives, while also facilitating quality control and radiologist training [11]–[14]. Nevertheless, their performance in liver MRI reporting remains heterogeneous across tasks and institutions, and two major challenges persist:

(1) *How can the credibility of LLM-generated radiology reports be objectively evaluated?* Existing approaches often depend on LLMs themselves for output quality assessment, which increases computational burden, limits real-time deployment, and necessitates additional prompts for evaluation. Moreover, such self-assessment methods risk perpetuating model bias and lack interpretability [15], [16]. Although human validation by radiologists

could enhance reliability, manually reviewing tens of thousands of reports is practically infeasible due to the immense workload and time constraints. To date, no standardized and objective framework has been established to assess the semantic integrity and diagnostic reliability of LLM-generated reports in a model-agnostic and reproducible manner [17].

(2) *How can LLMs be effectively guided to understand imaging findings and generate diagnostic conclusions through prompt design?* Although several studies have explored different prompting strategies, most remain highly task- or dataset-specific, and lack adaptability to institutional reporting styles. This limitation constrains generalizability and hampers clinical implementation across diverse environments. In the absence of well-established design principles, prompt engineering remains largely empirical, relying on iterative, trial-and-error approaches [18], [19].

To address these challenges, we developed a unified prompt design protocol compatible with multiple LLMs, and established an objective evaluation framework to assess the credibility and quality of LLM-generated radiology reports. Firstly, we systematically evaluate 11 customized prompting strategies—ranging from minimal to example-based and checklist-guided designs—to assess their influence on report reliability and consistency. Secondly, we further introduce a Multi-Dimensional Credibility Assessment (MDCA) framework that evaluates report quality across three clinically relevant dimensions: Semantic Coherence (SC), Diagnostic Correctness (DC), and Clinical Prioritization Alignment (CPA) [20], [21]. Finally, with the help of MDCA, multiple state-of-the-art Chinese LLMs, including Kimi-K2-Instruct-0905, Qwen3-235B-A22B-Instruct-2507, DeepSeek-V3, and ByteDance-Seed-OSS-36B-Instruct, are evaluated using the same platform to identify practical strategies that improve reporting quality, support radiology quality assurance, and facilitate trainee education [7], [9], [13], [22].

II. MATERIALS AND METHODS

This retrospective study was conducted at Department of Radiology, The First Affiliated Hospital

of Army Medical University. The requirement for informed consent was waived due to the use of de-identified patient data. Liver radiology reports without diagnostic conclusions were input to the LLMs between April 30, 2025, and May 14, 2025.

A. Collection of Clinical Reports

The collection process of clinical reports is shown in Figure 1. All reports were obtained from our center for patients who underwent Gd-EOB-DTPA-enhanced liver MRI between January and December 2024 ($n = 24,797$). Exclusion criteria included a history of hepatic surgery or any systemic anti-tumor therapy, a history of extrahepatic primary malignancy, absence of any benign or malignant hepatic lesions, and poor-quality MRI images that prevented reliable assessment. The review process yielded 15,127 eligible liver MRI reports for inclusion in the study.

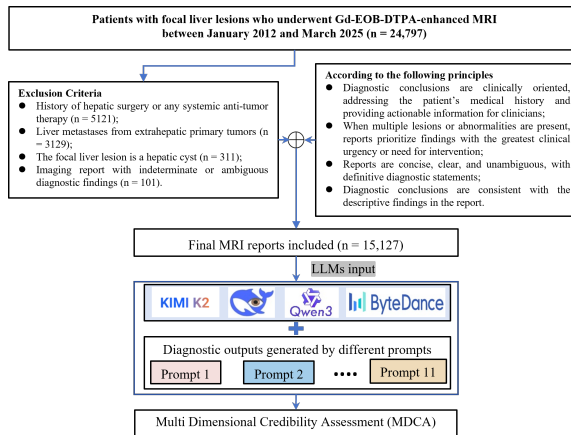


Fig. 1: The collection process of clinical reports. This process followed a well-designed exclusion criteria to ensure the quality and relevance of the reports used for LLM evaluation.

B. Multi-Dimensional Credibility Assessment Framework

To independently evaluate the synthesized reports, we proposed a MDCA framework, which evaluated the synthesized reports in three dimensions: SC, DC, and CPA [20], [21], [23], [24].

Semantic Coherence (SC): This metric assessed whether the generated report read fluently and adhered to typical radiological writing conventions. A pre-trained BERT model was used to compute pairwise sentence embeddings and evaluate overall coherence as follows:

$$SC = BERT(s_T, s_S) \quad (1)$$

where s_T was the target diagnosis sentence, s_S was the synthesized diagnosis sentence. Higher SC indicated smoother sentence transitions and better linguistic fluency, reflecting alignment with radiologists' reading habits. Importantly, this metric focused solely on textual coherence and did not assess the diagnostic accuracy of the liver MRI report.

Diagnostic Correctness (DC): This dimension evaluated the accuracy and completeness of diagnostic content. For each report R , we divided it into several diagnosis target $T_R = \{t_{R1}, t_{R2}, t_{R3}, \dots\}$. For target report R_T and synthesized report R_S , we had T_{RT} and T_{RS} . Then we conducted keyword matching KMAT between T_{RT} and T_{RS} , and each t_{RTo} would be compared with all t_{ST} . As a result, we have:

$$DC = KMAT(R_T, R_S) \quad (2)$$

Reports were scored based on disease coverage and terminology precision. A higher score reflected stronger diagnostic performance and clinical relevance [25]–[27].

Clinical Prioritization Alignment (CPA): This metric assessed whether the most clinically urgent or important findings were presented at the top of the report, consistent with real-world diagnostic priorities. For example, malignant tumors or acute conditions (e.g., hemorrhage) should have appeared at the very first. Scoring was based on whether such high-priority diagnoses appeared within the top 1, top 3, or top 5 positions in the report. Expert radiologists validated prioritization alignment according to institutional guidelines. Based on the clinical requirements in the Department of Radiology, The First Affiliated Hospital of Army Medical University, the calculation process was defined in two steps:

Step 1: t_{RT1} would be compared with t_{ST1} . If they match, a score of 1 was assigned; otherwise, the score was 0. Thus, the score for this step X_1 was either 1 or 0.;

Step2: each t_{RTo} would be compared with t_{STo-1} , t_{STo} , and t_{STo+1} , where $o > 1$, was the sentence number. For example, t_{RT2} would be matched with t_{RS1} , t_{RS2} , and t_{RS3} . This pattern continued accordingly. Each matched diagnosis was assigned a score of 1, and the total score was obtained by summing all matched instances. The total score for given reports was then normalized by dividing the number of matched diagnoses by the total number of candidate diagnoses, resulting in a final score X_2 between 0 and 1. The final CPA was calculated as:

$$CPA = 0.5 \times X_1 + 0.5 \times X_2 \quad (3)$$

In addition, Top-1 matching scores were calculated to further evaluate model performance in identifying the key diagnostic conclusions. A score of 1 was assigned when the model's primary diagnosis exactly matched the ground truth, and 0 otherwise. MDCA Score: The final MDCA score was defined as follow:

$$MDCA = 0.2 \times SC + 0.4 \times DC + 0.4 \times CPA \quad (4)$$

Generally, equal weights should be assigned to SC, DC, and CPA. However, SC—calculated using BERT—focuses primarily on textual coherence. In other words, it emphasizes whether the report reads like it was written by a local radiologist, rather than assessing diagnostic accuracy or clinical relevance. Therefore, the weight of SC may reasonably be set lower, as generating fluent and coherent text is relatively easy for LLMs.

C. Prompt Design and Implementation

As shown in Table I, the prompt content were categorized into two major types: instruction-based components, and example-based guidance. The instruction-based components contained (1) role specification, (2) task definition, (3) tiered diagnostic taxonomy (TOP system), (4) mandatory verification checkpoints, (5) report formatting standards, and (6) radiologic diagnostic principles. The

example-based component consisted of sample reports written by experienced radiologists, which provided reference style and diagnostic reasoning patterns.

To systematically evaluated the contribution of each component, 11 prompt combinations were developed by selectively integrating different elements from these categories. This design enabled quantitative assessment of how individual and combined prompt features influence the diagnostic reliability, coherence, and consistency of LLM-generated liver MRI reports. Full prompt formulations are provided in the Table II.

Prompts P0-P6 were designed to test different combinations of instruction-based and example-based components, enabling the identification of the most effective prompt composition strategy. Prompts P5-P11 were further used to examine how the number of examples influences model learning and output performance, thereby clarifying the role of sample augmentation in improving large language model adaptability and diagnostic consistency. We also provided the information for each prompt's character length in Table II.

D. Preparation of Large Language Models

Four advanced Chinese large language models (LLMs) were evaluated in this study: Kimi-K2-Instruct-0905 (Moonshot AI), Qwen3-235B-A22B-Instruct-2507 (Alibaba Group), DeepSeek-V3 (DeepSeek AI), and ByteDance-Seed-OSS-36B-Instruct (ByteDance). These models represent the leading generation of instruction-tuned Chinese LLMs, each trained on large-scale multimodal or text-based corpora and optimized for complex reasoning and task following [28], [29].

To further assess intra-model consistency, the DeepSeek family was additionally tested with its upgraded version DeepSeek-V3.1 and DeepSeek-R1 with Chain-of-Thought [30], [31]. This comparison allowed evaluation of how incremental model updates and explicit reasoning mechanisms affect diagnostic accuracy and report credibility in liver MRI interpretation.

All models were accessed and executed via standardized SiliconFlow APIs to ensure a consistent

TABLE I: Summary of Prompt Design Components and Example Content

| Component (EN) | Component (中文) | Example Content (EN / 中文) |
|---|----------------|---|
| Role Specification | 角色设定 | You are a radiologist with 30 years of experience in liver MRI interpretation, specializing in HCC and FNH ... 你是一名具有30年肝脏MRI诊断经验的腹部影像诊断医师，专长良恶性肝占位鉴别（尤其FNH/血管瘤/ICC/HCC）... |
| Task Definition | 基本任务要求 | Prioritize malignant tumors and avoid speculative conclusions. Follow diagnostic standards ... 强制优先诊断恶性肿瘤；禁止推测性结论，严格遵循诊断标准... |
| Tiered Diagnostic Taxonomy (TOP System) | 分级诊断体系 (TOP) | TOP1: HCC, ICC, metastases, ... TOP2: FNH, hemangioma, ... TOP3: Cirrhosis, portal hypertension, ... TOP4: Lymphadenopathy, biliary stones, ... TOP5: Renal cysts, pleural effusion, ... TOP1: HCC、胆管细胞癌、转移瘤等, ... TOP2: 局灶性结节增生、血管瘤等 TOP3: 肝硬化、门脉高压等 TOP4: 淋巴结增大、胆系结石等 TOP5: 肾囊肿、胸腔积液等 |
| Mandatory Checkpoints | 强制核查项 | Confirm HCC, metastases, perfusion anomalies, cirrhosis, lymphadenopathy, renal cysts, ... 肝癌 转移灶 灌注异常 肝硬化 淋巴结 肾囊肿等，每项需逐一确认。 |
| Report Formatting Standards | 报告结构规范 | Format: anatomical location + disease, one line per diagnosis, ordered by TOP level ... 格式：解剖部位+病变类型，每行为一条，按TOP顺序书写，等等 |
| Radiologic Diagnostic Principles | 影像诊断原则 | e.g., HCC: arterial enhancement, washout, hepatobiliary hypointensity ... 例如HCC：动脉期强化，门脉期或延迟期洗脱，肝胆期低信号等 |
| Example Report | 样例报告 | Findings: Liver shows irregular margins and a 4.2×3.3 cm lesion in Segment IVb. Arterial rim enhancement with washout; hypointense on hepatobiliary phase. Enlarged periportal lymph nodes. Diagnosis: 1. Segment IVb lesion suggestive of HCC. 2. Cirrhosis with portal hypertension. 3. Enlarged lymph nodes, metastasis cannot be excluded. 检查所见：肝IVb段见团块状占位，动脉期环形强化，延迟期洗脱，肝胆期低信号，肝门部淋巴结增大。 结论：1. 肝IVb段占位，考虑HCC可能。2. 肝硬化伴门脉高压。3. 肝门部淋巴结增大，转移不排除。 |

TABLE II: Composition Matrix of the 11 Prompt Configurations.

| Prompt ID | Role Definition | Core Task Specification | TOP Diagnostic Taxonomy | Mandatory Verification Items | Report Structure Standards | Imaging Diagnostic Principles | Number of Examples | Character Length (Chinese) |
|-----------|-----------------|-------------------------|-------------------------|------------------------------|----------------------------|-------------------------------|--------------------|----------------------------|
| Prompt 0 | ✓ | - | - | - | - | - | 0 | 124 |
| Prompt 1 | ✓ | ✓ | - | - | - | - | 0 | 270 |
| Prompt 2 | ✓ | ✓ | - | - | - | - | 3 | 1411 |
| Prompt 3 | ✓ | ✓ | ✓ | - | ✓ | - | 3 | 2036 |
| Prompt 4 | ✓ | ✓ | ✓ | ✓ | ✓ | ✓ | 3 | 3147 |
| Prompt 5 | ✓ | ✓ | - | - | - | - | 10 | 3946 |
| Prompt 6 | ✓ | ✓ | ✓ | ✓ | ✓ | ✓ | 10 | 5709 |
| Prompt 7 | ✓ | ✓ | ✓ | ✓ | ✓ | ✓ | 0 | 2104 |
| Prompt 8 | ✓ | ✓ | ✓ | ✓ | ✓ | ✓ | 5 | 3953 |
| Prompt 9 | ✓ | ✓ | ✓ | ✓ | ✓ | ✓ | 15 | 7609 |
| Prompt 10 | ✓ | ✓ | ✓ | ✓ | ✓ | ✓ | 20 | 9457 |
| Prompt 11 | ✓ | ✓ | ✓ | ✓ | ✓ | ✓ | 25 | 11025 |

computational environment and to minimize confounding factors related to hardware or deployment variability. The parameter *enable_thinking* (if applicable) was uniformly set to *False* to disable the models' internal "thinking" function, as long conversational contexts were not considered in this study. The parameters *temperature*, *top_p*, and *max_tokens* were set to 0.5, 0.95, and 1024, respectively.

III. RESULTS

The results are presented in three parts, corresponding to the experimental workflow. First, DeepSeek-V3 and Kimi-K2 were used to illustrate how different prompt compositions affect model performance. Second, these two models were further applied to evaluate the influence of varying the number of example reports on report quality. Finally, we compared multiple Chinese large language models and validated the DeepSeek family to clarify why DeepSeek-V3 and Kimi-K2 were selected as representative models for subsequent experiments. In addition, we aimed to demonstrate that the designed prompt settings yielded consistent performance patterns across different models, supporting the generalizability of the proposed approach.

A. Effect of Prompt Composition on Model Performance

In this section, DeepSeek-V3 and Kimi-K2 were evaluated using Prompts P0-P6, as detailed in Table 1. For each prompt configuration, a total of 15,127 liver MRI reports were tested, corresponding to 181,524 chat sessions conducted through the LLM interfaces.

As shown in Figure 2 and Table III, which present the experimental results for prompt designs with Kimi-K2 and DeepSeek-V3, Kimi-K2 consistently outperformed DeepSeek-V3 across all prompt settings. Kimi-K2 with Prompt 6 achieved the highest scores in Semantic Coherence (SC), Clinical Prioritization Alignment (CPA), and overall MDCA, whereas Kimi-K2 with Prompt 4 yielded the best Diagnostic Correctness (DC) and Top-1 matching scores. Performance trends between the two LLMs were highly consistent across all prompt configurations. In addition, higher mean values were accompanied by lower standard deviations, indicating stable model behavior.

Overall, three major observations were identified.

First, prompts that included role definition but lacked explicit diagnostic guidance performed poorly, and those containing only role definition and

core task specification without structured support achieved even lower scores (Prompts 0 and 1).

Second, compared with instruction-only prompts, the inclusion of example-based guidance substantially improved overall performance (Prompts 1, 2, 5, and 4, 6), although this required greater token consumption and communication overhead.

Finally, the integration of key instruction-based components—specifically the tiered diagnostic taxonomy, mandatory verification items, report structure standards, and imaging diagnostic principles—further enhanced SC, DC, and Top-1 matching scores, leading to more accurate and diagnostically reliable outputs (Prompts 3, 4, and 5, 6).

B. Effect of Example Number on Model Performance

In this section, DeepSeek-V3 and Kimi-K2 were evaluated using Prompts 4 and 6-11. When sorted by the number of examples, these correspond to Prompts 7, 4, 8, 6, 9, 10, and 11, which contained 0, 3, 5, 10, 15, and 20 examples, respectively. For each prompt configuration, a total of 5,000 liver MRI reports were tested, corresponding to 70,000 chat sessions conducted through the LLM interfaces. The experimental results are summarized in Figure 3 and Table IV.

Both Kimi-K2 and DeepSeek-V3 exhibited consistent improvement across all evaluation dimensions as the number of examples increased. Performance gains were most notable in Semantic Coherence (SC) and Top-1 matching accuracy, indicating that additional examples enhanced the models' ability to generate fluent, contextually coherent, and diagnostically aligned reports.

Model performance increased steadily up to approximately 20 examples, beyond which further expansion yielded marginal or slightly negative effects. The composite score for DeepSeek-V3 peaked at 76.13 (Prompt 10), while Kimi-K2 reached 76.96 (Prompt 11), after which performance plateaued. Overall, the improvements beyond 20 examples were limited. These findings suggest that while moderate example augmentation—around 10 to 20 examples—substantially improves language fluency and diagnostic completeness, excessive examples

may introduce contextual noise and redundancy that hinder performance.

Notably, both models followed highly similar trends across all metrics, confirming that the effect of example number is consistent and model-agnostic. This consistency suggests that the observed performance gains stem from the underlying optimization of contextual understanding rather than model-specific characteristics, thereby supporting the generalizability of this prompt-scaling strategy across Chinese LLMs.

Finally, when instruction-based components are limited, we believe expanding the number of examples provides an effective alternative for improving performance, albeit with higher token and communication costs. In practical deployment, we recommend using a comprehensive instruction-based prompt design combined with approximately 10-15 representative examples, which offers an optimal balance between performance, efficiency, and feasibility for most clinical institutions.

C. Comparison of Chinese LLMs and Validation within the DeepSeek Family

In this section, four major Chinese large language models—Kimi-K2-Instruct-0905, DeepSeek-V3, ByteDance-Seed-OSS-36B-Instruct, and Qwen3-235B-A22B-Instruct-2507—were evaluated under prompt configurations of varying complexity (Prompts 2, 4, and 6). For each model-prompt combination, 7,500 liver MRI reports were tested, resulting in approximately 90,000 chat sessions conducted through the SiliconFlow platform. Experimental results are summarized in Figure 4.

All models demonstrated consistent performance gains with increasing prompt sophistication, highlighting the crucial role of structured instruction and contextual guidance. Kimi-K2 achieved the best overall performance, with composite scores improving from 72.71 (Prompt 2) to 76.15 (Prompt 6). DeepSeek-V3 followed closely, reaching 75.41 under the same condition. In contrast, ByteDance-Seed and Qwen3-235B showed limited improvements, particularly in Semantic Coherence (SC) and Clinical Prioritization Alignment (CPA), indicating weaker adaptability to complex prompt instructions.

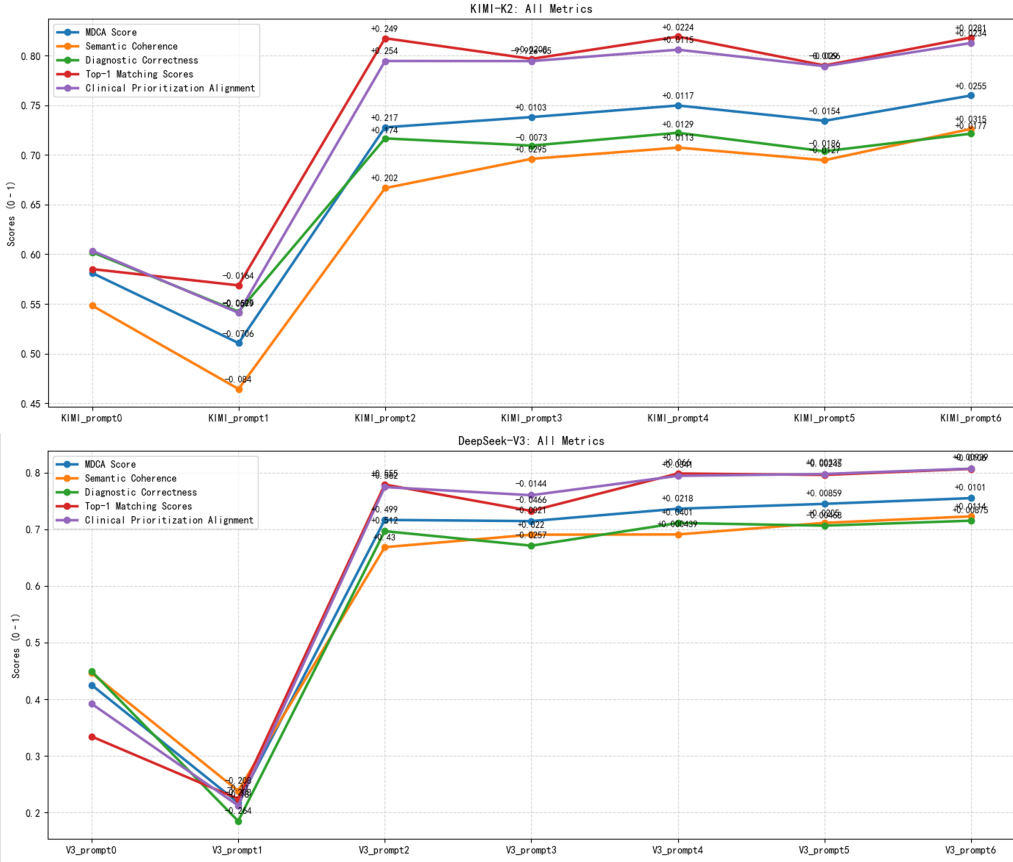


Fig. 2: Experimental results for Prompt Designs with KIMI-K2 and DeepSeek-V3. The figure illustrates the performance of both models across various prompt configurations, highlighting the impact of different prompt components on Semantic Coherence (SC), Diagnostic Correctness (DC), Top-1 matching, Clinical Prioritization Alignment (CPA), and overall MDCA scores.

Further validation within the DeepSeek family was conducted using 2,500 liver MRI reports per model-prompt configuration, enabling detailed comparison among DeepSeek-V3, DeepSeek-V3.1, and DeepSeek-R1. As shown in Figure 5, DeepSeek-V3 achieved the highest composite score (76.33), outperforming V3.1 (75.55) and R1 (74.33). While V3.1 exhibited marginally higher Semantic Coherence (0.730 vs. 0.725), V3 demonstrated superior Diagnostic Correctness (DC), Top-1 matching accuracy, and CPA, producing more diagnostically reliable reports. The reasoning-augmented R1 achieved slightly higher semantic correctness (0.715) but at

the cost of reduced consistency and fluency. These findings indicate that explicit Chain-of-Thought reasoning does not necessarily enhance clinical reliability, and that optimized instruction design remains more impactful for structured diagnostic generation.

Overall, both Kimi-K2 and DeepSeek-V3 emerged as the most reliable and balanced performers, consistently benefiting from prompt and sample optimization. The performance patterns across all models—characterized by steady improvement with increased instruction richness—demonstrate the model-agnostic generalizability of the proposed prompt

TABLE III: Evaluation Metrics for KIMI-K2 and DeepSeek-V3 with Different Prompt Designs.

| KIMI Mean(STD) | Prompt 0 | Prompt 1 | Prompt 2 | Prompt 3 | Prompt 4 | Prompt 5 | Prompt 6 |
|-----------------------|--------------------|--------------------|--------------------|--------------------|--------------------|--------------------|--------------------|
| SC | 0.5483 (0.2651) | 0.4643 (0.251) | 0.6666 (0.1966) | 0.6961 (0.1962) | 0.7073 (0.1925) | 0.6947 (0.1967) | 0.7262 (0.191) |
| DC | 0.6021 (0.3352) | 0.5422 (0.3708) | 0.7167 (0.2752) | 0.7094 (0.2799) | 0.7223 (0.2725) | 0.7036 (0.2839) | 0.7214 (0.2742) |
| Top-1 | 0.5851 (0.4927) | 0.5687 (0.4953) | 0.8175 (0.3863) | 0.7967 (0.4025) | 0.8191 (0.3849) | 0.7901 (0.4073) | 0.8182 (0.3857) |
| CPA | 0.6035 (0.3995) | 0.541 (0.41) | 0.7945 (0.2982) | 0.7944 (0.3028) | 0.8059 (0.2892) | 0.7893 (0.3019) | 0.8127 (0.2867) |
| MDCA | 0.5812 | 0.5106 | 0.7278 | 0.7381 | 0.7498 | 0.7343 | 0.7598 |
| Score | (0.2834) | (0.2878) | (0.1907) | (0.1954) | (0.1865) | (0.1949) | (0.1869) |
| DeepSeek Mean(STD) | Prompt 0 | Prompt 1 | Prompt 2 | Prompt 3 | Prompt 4 | Prompt 5 | Prompt 6 |
| SC | 0.4462 (0.2436) | 0.2381 (0.3157) | 0.6683 (0.1952) | 0.6903 (0.1952) | 0.6908 (0.1948) | 0.7112 (0.1947) | 0.7227 (0.1914) |
| DC | 0.4492 (0.3596) | 0.1848 (0.3065) | 0.6966 (0.2879) | 0.6709 (0.2995) | 0.711 (0.282) | 0.7063 (0.2844) | 0.7151 (0.2806) |
| Top-1 | 0.334 (0.4717) | 0.2239 (0.4169) | 0.7789 (0.415) | 0.7323 (0.4428) | 0.7983 (0.4013) | 0.7959 (0.4031) | 0.8065 (0.3951) |
| CPA | 0.3918 (0.3804) | 0.2121 (0.3612) | 0.7744 (0.3128) | 0.76 (0.3232) | 0.7942 (0.3009) | 0.7975 (0.2976) | 0.8069 (0.2927) |
| MDCA | 0.4250 | 0.2170 | 0.7164 | 0.7143 | 0.7362 | 0.7448 | 0.7548 |
| Score | (0.2667) | (0.3066) | (0.1973) | (0.2051) | (0.1922) | (0.1928) | (0.1894) |

customization and credibility evaluation frameworks. Consequently, these two models were selected as representative systems for subsequent experiments, reflecting their strong baseline capability, responsiveness to structured prompting, and robustness across diverse evaluation dimensions.

D. Consistency Check between MDCA Framework and Radiologist Judgments

To evaluate the clinical alignment of the MDCA framework, we conducted a consistency check between MDCA scores and radiologist assessments. Four representative prompts (Prompt 0, 2, 4, and 6) from Kimi-K2 were selected for comparison. Two board-certified radiologists independently reviewed 100 reports per prompt, totaling 800 reports, comparing each LLM-generated report against the corresponding ground-truth report.

Each report was rated using a three-tier scale:

Grade A (1 point): Fully acceptable, with clinically sound content and no major errors; Grade B (0.5 points): Acceptable with minor, tolerable issues (e.g., slightly ambiguous phrasing or minor inconsistencies); Grade C (0 points): Unacceptable due to incoherent language or critical factual inaccuracies. Each report received two individual ratings, and the combined score served as the final consistency judgment. Scores of 2.0 were considered excellent, 1.0-1.5 acceptable, and ≤ 1 unacceptable.

As illustrated in Figure 6, the proportion of reports rated as excellent (score = 2.0) increased substantially with improved prompt quality, from Prompt 0 to Prompt 6. In contrast, lower-quality prompts yielded a higher proportion of partially or wholly unacceptable outputs. These trends closely aligned with the MDCA scores, supporting the clinical validity and interpretability of the proposed framework.

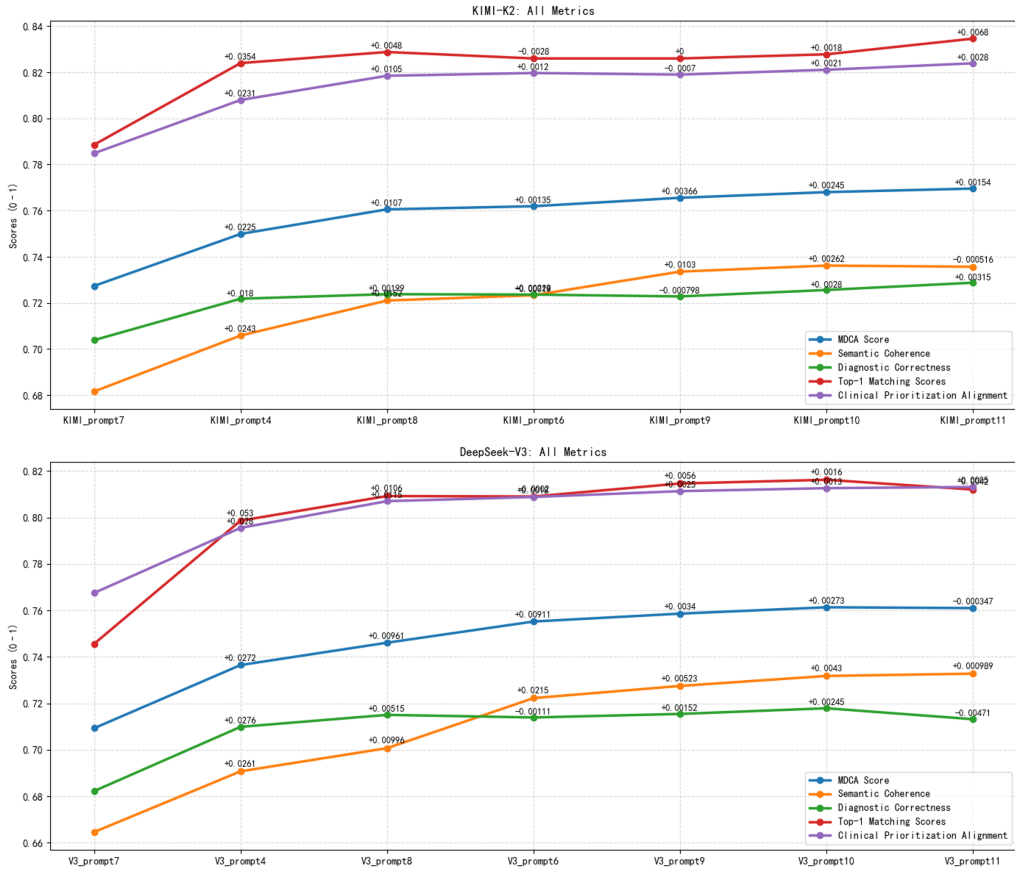


Fig. 3: Experimental Results with Different Example Numbers. The figure illustrates how varying the number of example reports in the prompts affects the performance of KIMI-K2 and DeepSeek-V3 across multiple evaluation metrics, including Semantic Coherence (SC), Diagnostic Correctness (DC), Top-1 matching, Clinical Prioritization Alignment (CPA), and overall MDCA scores.

Manual consistency checks, however, are labor-intensive and not scalable at the population level, further underscoring the need for automated, reproducible frameworks such as MDCA.

IV. DISCUSSION

A. Prompt Design Principles and Mechanistic Insights

Our findings highlight that prompt construction in large language model (LLM)-based radiology reporting is not merely additive but synergistic. Instruction-based components—including role definition, core task specification, tiered diagnostic tax-

onomy (TOP system), mandatory verification items, report structure standards, and imaging diagnostic principles—substantially improved Diagnostic Correctness (DC) and Clinical Prioritization Alignment (CPA) by enforcing structured reasoning and domain-specific consistency. In contrast, the inclusion of example-based guidance primarily enhanced Semantic Coherence (SC), promoting fluency and logical continuity in report narratives. However, excessive examples (≥ 20) introduced contextual redundancy and token interference, resulting in performance saturation or mild decline. These results suggest that an optimal balance—combining com-

TABLE IV: Evaluation Metrics for KIMI-K2 and DeepSeek-V3 with Different Example Numbers.

| KIMI Mean(STD) | Prompt 7 | Prompt 4 | Prompt 8 | Prompt 6 | Prompt 9 | Prompt 10 | Prompt 11 |
|-----------------------|--------------------|--------------------|--------------------|--------------------|--------------------|--------------------|--------------------|
| SC | 0.6816 (0.1934) | 0.7058 (0.1925) | 0.721 (0.1906) | 0.7233 (0.1922) | 0.7335 (0.1898) | 0.7362 (0.189) | 0.7357 (0.1887) |
| DC | 0.7038 (0.2826) | 0.7218 (0.2701) | 0.7238 (0.2704) | 0.7236 (0.2697) | 0.7228 (0.2716) | 0.7256 (0.2692) | 0.7287 (0.2682) |
| Top-1 | 0.7886 (0.4084) | 0.824 (0.3809) | 0.8288 (0.3768) | 0.826 (0.3792) | 0.826 (0.3792) | 0.8278 (0.3776) | 0.8346 (0.3716) |
| CPA | 0.7849 (0.3084) | 0.808 (0.2891) | 0.8185 (0.2822) | 0.8197 (0.2842) | 0.819 (0.2824) | 0.8211 (0.2808) | 0.8239 (0.2796) |
| MDCA | 0.7273 | 0.7500 | 0.7605 | 0.7619 | 0.7656 | 0.7680 | 0.7696 |
| Score | (0.1981) | (0.1856) | (0.1834) | (0.1852) | (0.1839) | (0.1826) | (0.1812) |
| DeepSeek Mean(STD) | Prompt 7 | Prompt 4 | Prompt 8 | Prompt 6 | Prompt 9 | Prompt 10 | Prompt 11 |
| SC | 0.6646 (0.194) | 0.6907 (0.1943) | 0.7007 (0.1927) | 0.7222 (0.1895) | 0.7275 (0.1923) | 0.7318 (0.1918) | 0.7328 (0.1935) |
| DC | 0.6822 (0.2932) | 0.7099 (0.2805) | 0.715 (0.2789) | 0.7139 (0.2796) | 0.7154 (0.2775) | 0.7179 (0.2765) | 0.7132 (0.279) |
| Top-1 | 0.7456 (0.4356) | 0.7986 (0.4011) | 0.8092 (0.393) | 0.809 (0.3931) | 0.8146 (0.3887) | 0.8162 (0.3874) | 0.812 (0.3908) |
| CPA | 0.7675 (0.3189) | 0.7955 (0.2982) | 0.807 (0.2929) | 0.8088 (0.2916) | 0.8113 (0.2884) | 0.8126 (0.2871) | 0.8131 (0.2885) |
| MDCA | 0.7093 | 0.7365 | 0.7461 | 0.7552 | 0.7586 | 0.7613 | 0.7610 |
| Score | (0.2041) | (0.1902) | (0.1886) | (0.1881) | (0.1874) | (0.1865) | (0.1889) |

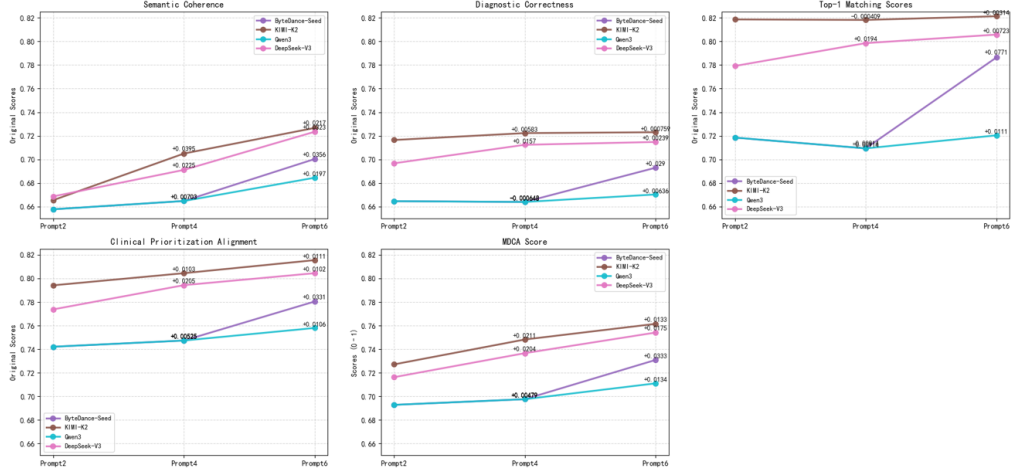


Fig. 4: Experimental Results with Four LLMs. The figure illustrates the performance of KIMI-K2, DeepSeek-V3, ByteDance-Seed, and Qwen3-235B across various prompt configurations.

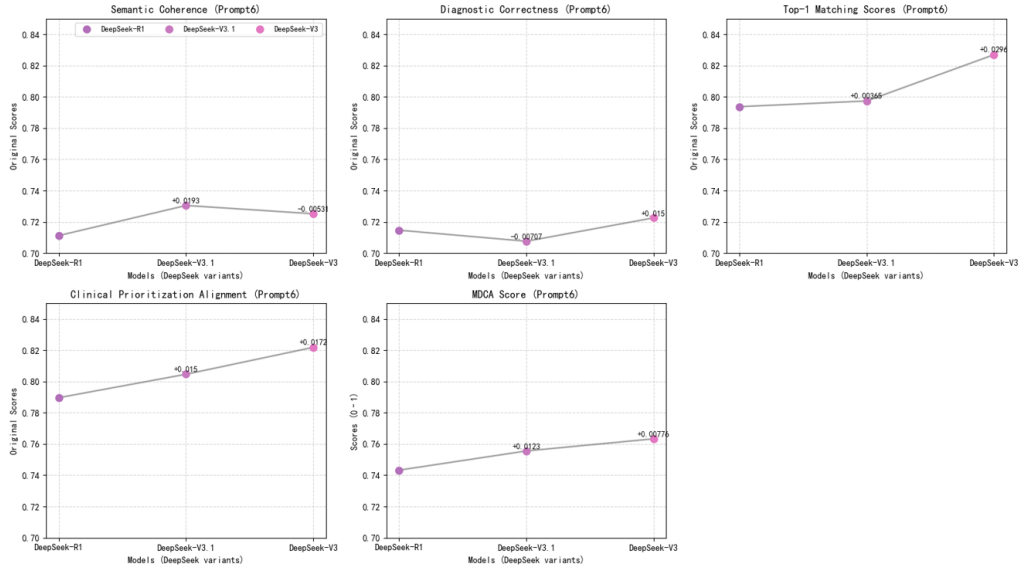


Fig. 5: Experimental Results with DeepSeek Family. The figure illustrates the performance of DeepSeek-V3, DeepSeek-V3.1, and DeepSeek-R1 across various prompt configurations.

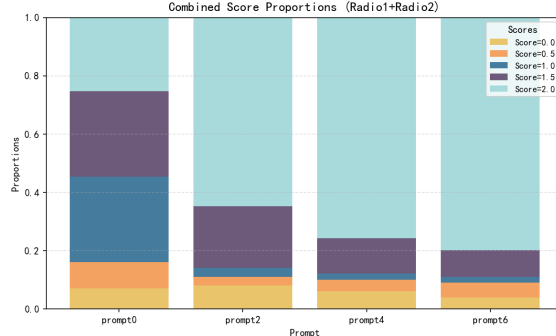


Fig. 6: Combined Scores and Proportions of Radiologist Ratings for KIMI-K2 under Different Prompts. The figure illustrates the distribution of radiologist ratings (Grade A, B, C) for KIMI-K2-generated reports across four prompt configurations (Prompt 0, 2, 4, and 6), highlighting the correlation between prompt quality and clinical acceptability.

prehensive instruction design with approximately 10-15 representative examples—achieves the best trade-off between diagnostic accuracy, fluency, and computational efficiency.

B. Model Performance and Selection Considerations

Among the evaluated models, Kimi-K2 and DeepSeek-V3 consistently outperformed other Chinese LLMs, exhibiting strong baseline reliability and responsiveness to prompt optimization. Within the DeepSeek family, V3 achieved the most balanced and diagnostically consistent performance, surpassing both V3.1 and the reasoning-augmented R1 variant. While V3.1 showed slightly higher semantic coherence, and R1 demonstrated marginal gains in correctness, neither delivered stable improvements across diagnostic metrics. These findings indicate that the integration of explicit reasoning mechanisms does not necessarily translate to higher clinical reliability, whereas structured prompt optimization has a more direct and reproducible effect.

Importantly, the consistent response patterns observed across all models demonstrate the generalizability of the proposed prompt design protocols. This cross-model stability suggests that scientifically designed prompts exert a greater influence on report quality than model selection itself. In

other words, the reliability and trustworthiness of LLM-generated radiology reports depend more on how models are instructed than on which models are used—underscoring the central role of prompt engineering in clinical LLM deployment.

C. Practical Applications and Clinical Implications

Beyond technical performance, the proposed frameworks hold strong potential for real-world applications in radiology workflows. The Multi-Dimensional Credibility Assessment (MDCA) system provides an interpretable and quantitative basis for quality control, allowing automated benchmarking of report consistency, diagnostic accuracy, and adherence to institutional standards. Such a framework could be integrated into hospital reporting systems to assist in automated quality assurance and longitudinal monitoring of reporting performance.

The MDCA framework offers several distinct advantages over existing single-metric or LLM-based self-evaluation approaches. First, it evaluates model outputs across three complementary dimensions—Semantic Coherence (SC), Diagnostic Correctness (DC), and Clinical Prioritization Alignment (CPA)—capturing both linguistic and clinical reliability within a unified structure; Second, the framework is model-agnostic, enabling fair comparison among different LLMs without dependence on internal architectures or training data; Third, each dimension is interpretable and directly maps to radiological reasoning processes, allowing human experts to trace and validate model errors. Together, these features make MDCA a practical, transparent, and reproducible tool for continuous model evaluation and regulatory oversight.

From an educational perspective, the prompt optimization and credibility evaluation frameworks can also support radiology trainee education. LLM-generated reports, when aligned with expert-verified prompts, can serve as high-quality exemplars to improve trainees' diagnostic reasoning, linguistic precision, and report standardization. This dual application—quality control and education—demonstrates the broader clinical and pedagogical value of trustworthy LLM deployment in medical imaging.

V. LIMITATIONS

This study has several limitations.

First, it focused exclusively on text-to-text large language models (LLMs) rather than multimodal systems capable of directly processing imaging data. While multimodal models hold promise for integrating visual and textual reasoning, they currently face deployment barriers related to high GPU requirements, complex DICOM handling, and limited clinical infrastructure. In contrast, text-based frameworks such as DeepSeek-V3 and Kimi-K2 provide a more practical and scalable alternative, particularly for resource-constrained healthcare institutions.

Second, the evaluation involved only radiologists, without incorporating feedback from other clinical specialists such as surgeons or oncologists. Although this focus ensured domain consistency, it may have limited the comprehensiveness of the credibility assessment (MDCA) in capturing broader multidisciplinary perspectives. Future studies could include multi-specialty panels to refine and expand the interpretive dimensions of the MDCA framework.

Finally, the single-center design may restrict generalizability. Model behaviors and prompt effectiveness could vary across institutions with different reporting styles and linguistic norms. Larger multicenter and longitudinal studies are warranted to validate the reproducibility and scalability of the proposed prompt optimization and credibility evaluation frameworks in diverse real-world settings.

VI. CONCLUSIONS

This study introduces a Multi-Dimensional Credibility Assessment (MDCA) framework that enables objective, transparent, and reproducible evaluation of LLM-generated liver MRI reports. Using this framework, we systematically investigated how scientific prompt design and model selection influence report quality. The findings indicate that structured instruction with approximately 10-15 representative examples achieve the most balanced and reliable performance. Among the evaluated models, Kimi-K2 and DeepSeek-V3 consistently demonstrated superior overall credibility. These results underscore

that both rational prompt engineering and credible model evaluation are essential for integrating trustworthy large language models into radiology workflows for quality assurance and professional training.

REFERENCES

- [1] J. M. Llovet, F. Castet, M. Heikenwalder, M. K. Maini, V. Mazzaferro, D. J. Pinato, E. Pikarsky, A. X. Zhu, and R. S. Finn, “Immunotherapies for hepatocellular carcinoma,” *Nature reviews Clinical oncology*, vol. 19, no. 3, pp. 151–172, 2022.
- [2] J. Bruix and M. Sherman, “Management of hepatocellular carcinoma,” *Hepatology*, vol. 42, no. 5, pp. 1208–1236, 2005.
- [3] A. Vogel, T. Meyer, G. Sapisochin, R. Salem, and A. Saborowski, “Hepatocellular carcinoma,” *The Lancet*, vol. 400, no. 10360, pp. 1345–1362, 2022. [Online]. Available: <https://www.sciencedirect.com/science/article/pii/S0140673622012004>
- [4] T. Aoki, N. Nishida, K. Ueshima, M. Morita, H. Chishina, M. Takita, S. Hagiwara, H. Ida, Y. Minami, A. Yamada *et al.*, “Higher enhancement intrahepatic nodules on the hepatobilary phase of gd-eob-dtpa-enhanced mri as a poor responsive marker of anti-pd-1/pd-11 monotherapy for unresectable hepatocellular carcinoma,” *Liver Cancer*, vol. 10, no. 6, pp. 615–628, 2021.
- [5] Z. Ye, J. Zhao, D. Hu, Z. Yang, J. Chen, L. Xu, Z. Zhou, M. Chen, and Y. Zhang, “Gd-eob-dtpa-enhanced mri proves advantageous in selecting surgical candidates for patients with early-stage hepatocellular carcinoma: An analysis in terms of oncological outcomes,” *iLIVER*, vol. 3, no. 4, p. 100117, 2024.
- [6] X. Wu, Y. Huang, and Q. He, “A large language model improves clinicians’ diagnostic performance in complex critical illness cases,” *Critical Care*, vol. 29, no. 1, p. 230, 2025.
- [7] K. Team, Y. Bai, Y. Bao, G. Chen, J. Chen, N. Chen, R. Chen, Y. Chen, Y. Chen, Y. Chen *et al.*, “Kimi k2: Open agentic intelligence,” *arXiv preprint arXiv:2507.20534*, 2025.
- [8] A. Yang, A. Li, B. Yang, B. Zhang, B. Hui, B. Zheng, B. Yu, C. Gao, C. Huang, C. Lv *et al.*, “Qwen3 technical report,” *arXiv preprint arXiv:2505.09388*, 2025.
- [9] B. Seed, J. Chen, T. Fan, X. Liu, L. Liu, Z. Lin, M. Wang, C. Wang, X. Wei, W. Xu *et al.*, “Seed1. 5-thinking: Advancing superb reasoning models with reinforcement learning,” *arXiv preprint arXiv:2504.13914*, 2025.
- [10] P. Chen, X. Liu, Z. Liu, Z. Chen, X. Zhang, H. Hu, Z. Wang, K. Wang, S. Shi, and S. Lian, “Fuzzy reasoning chain: An innovative reasoning framework from fuzziness to clarity,” *arXiv preprint arXiv:2509.22054*, 2025.
- [11] F. Gaber, M. Shaik, F. Allega, A. J. Bilecz, F. Busch, K. Goon, V. Franke, and A. Akalin, “Evaluating large language model workflows in clinical decision support for triage and referral and diagnosis,” *npj Digital Medicine*, vol. 8, no. 1, p. 263, 2025.
- [12] C. Marrocchio and N. Sverzellati, “Will generative large language models become radiologists’ invaluable allies?” p. e251259, 2025.
- [13] S. Sandmann, S. Heggemann, M. Fujarski, L. Bickmann, B. Wild, R. Eils, and J. Varghese, “Benchmark evaluation of deepseek large language models in clinical decision-making,” *Nature Medicine*, pp. 1–1, 2025.
- [14] M. Tordjman, Z. Liu, M. Yuce, V. Fauveau, Y. Mei, J. Hadadj, I. Bolger, H. Almansour, C. Horst, A. S. Parihar *et al.*, “Comparative benchmarking of the deepseek large language model on medical tasks and clinical reasoning,” *Nature medicine*, pp. 1–1, 2025.
- [15] L. Folio, L. Machado, and A. Dwyer, “Multimedia-enhanced radiology reports: Concept, components, and challenges,” *RadioGraphics*, vol. 38, pp. 462–482, 03 2018.
- [16] Y. Wang, E. Courcelles, E. Peyronnet, S. Porte, A. Diatchenko, E. Jacob, D. Angoulvant, P. Amarenco, F. Boccaro, B. Cariou *et al.*, “Credibility assessment of a mechanistic model of atherosclerosis to predict cardiovascular outcomes under lipid-lowering therapy,” *npj Digital Medicine*, vol. 8, no. 1, p. 171, 2025.
- [17] T. Tu, M. Schaeckermann, A. Palepu, K. Saab, J. Freyberg, R. Tanno, A. Wang, B. Li, M. Amin, Y. Cheng *et al.*, “Towards conversational diagnostic artificial intelligence,” *Nature*, pp. 1–9, 2025.
- [18] T. T. Kim, M. Makutonin, R. Sirous, and R. Javan, “Optimizing large language models in radiology and mitigating pitfalls: prompt engineering and fine-tuning,” *RadioGraphics*, vol. 45, no. 4, p. e240073, 2025.
- [19] M. A. Fink, A. Bischoff, C. A. Fink, M. Moll, J. Kroschke, L. Dulz, C. P. Heubel, H.-U. Kauczor, and T. F. Weber, “Potential of chatgpt and gpt-4 for data mining of free-text ct reports on lung cancer,” *Radiology*, vol. 308, no. 3, p. e231362, 2023.
- [20] Y. Zhou, L. Huang, T. Zhou, H. Fu, and L. Shao, “Visual-textual attentive semantic consistency for medical report generation,” in *Proceedings of the IEEE/CVF International Conference on Computer Vision*, 2021, pp. 3985–3994.
- [21] J. Chen, G. Huang, X. Yuan, G. Zhong, Z. Tan, C.-M. Pun, and Q. Yang, “Visual-linguistic diagnostic semantic enhancement for medical report generation,” *Journal of Biomedical Informatics*, vol. 161, p. 104764, 2025.
- [22] J. Chou, A. Liu, Y. Deng, Z. Zeng, T. Zhang, H. Zhu, J. Cai, Y. Mao, C. Zhang, L. Tan *et al.*, “Autocodebench: Large language models are automatic code benchmark generators,” *arXiv preprint arXiv:2508.09101*, 2025.
- [23] D. Zeng, Y. Qin, B. Sheng, and T. Y. Wong, “Deepseek’s “low-cost” adoption across china’s hospital systems: Too fast, too soon?” *Jama*, vol. 333, no. 21, pp. 1866–1869, 2025.
- [24] R. Bhayana, B. Nanda, T. Dehkharghanian, Y. Deng, N. Bhambra, G. Elias, D. Datta, A. Kambadakone, C. G. Shwartz, C.-A. Moulton *et al.*, “Large language models for automated synoptic reports and resectability categorization in pancreatic cancer,” *Radiology*, vol. 311, no. 3, p. e233117, 2024.
- [25] C. H. Savage, G. Chaudhari, A. D. Smith, and J. H. Sohn, “Radsearch, a semantic search model for accurate radiology report retrieval with large language model integration,” *Radiology*, vol. 315, no. 1, p. e240686, 2025.

- [26] K. Yasaka and O. Abe, “A new step forward in the extraction of appropriate radiology reports,” p. e250867, 2025.
- [27] A. Lucas, T. C. Arnold, S. V. Okar, C. Vadali, K. D. Kawatra, Z. Ren, Q. Cao, R. T. Shinohara, M. K. Schindler, K. A. Davis *et al.*, “Multisquence 3-t image synthesis from 64-mt low-field-strength mri using generative adversarial networks in multiple sclerosis,” *Radiology*, vol. 315, no. 1, p. e233529, 2025.
- [28] Z. Zhang, Y. Yao, A. Zhang, X. Tang, X. Ma, Z. He, Y. Wang, M. Gerstein, R. Wang, G. Liu *et al.*, “Igniting language intelligence: The hitchhiker’s guide from chain-of-thought reasoning to language agents,” *ACM Computing Surveys*, vol. 57, no. 8, pp. 1–39, 2025.
- [29] Q. Lyu, S. Havaldar, A. Stein, L. Zhang, D. Rao, E. Wong, M. Apidianaki, and C. Callison-Burch, “Faithful chain-of-thought reasoning,” in *The 13th International Joint Conference on Natural Language Processing and the 3rd Conference of the Asia-Pacific Chapter of the Association for Computational Linguistics (IJCNLP-AACL 2023)*, 2023.
- [30] C. Zhao, C. Deng, C. Ruan, D. Dai, H. Gao, J. Li, L. Zhang, P. Huang, S. Zhou, S. Ma *et al.*, “Insights into deepseek-v3: Scaling challenges and reflections on hardware for ai architectures,” in *Proceedings of the 52nd Annual International Symposium on Computer Architecture*, 2025, pp. 1731–1745.
- [31] L. Chan, X. Xu, and K. Lv, “Deepseek-r1 and gpt-4 are comparable in a complex diagnostic challenge: a historical control study,” *International Journal of Surgery*, vol. 111, no. 6, pp. 4056–4059, 2025.